Aspergillus terreus Broth Rheology, Oxygen Transfer, and Lovastatin Production in a Gas-Agitated Slurry Reactor

E. M. Rodríguez Porcel,[†] J. L. Casas López,*[,†] J. A. Sánchez Pérez,[†] J. M. Fernández Sevilla,[†] J. L. García Sánchez,[†] and Y. Chisti[‡]

Department of Chemical Engineering, University of Almería, 04120 Almería, Spain, and Institute of Technology and Engineering, Massey University, Private Bag 11 222, Palmerston North, New Zealand

A 20 L gas-agitated slurry bubble column bioreactor was used to investigate the effects of nonmechanical low-intensity agitation on development of broth rheology and fungal pellet morphology during production of lovastatin by the filamentous fungus *Aspergillus terreus*. Fermentations were carried out under elevated dissolved oxygen levels (400% of air saturation) at gassing rates that ranged from 0.5 to 1.5 vvm. Various initial concentrations of the growth limiting nitrogen source were used to attain different total biomass concentrations, to observe the effect of this variable on development of pellets and the rheology of the fermentation broth. The non-Newtonian rheology of the fermentation broth was influenced both by the biomass concentration and the size of the fungal pellets. The stable pellet diameter ranged from ∼2300 to ∼2900 μm. Too low turbulence (gassing rate of 0.5 vvm) and low dissolved oxygen levels adversely affected lovastatin production. The best biomass specific production of lovastatin was attained at high biomass concentrations under oxygen-rich conditions that were not excessively turbulent. In fermentation broths with various rheologies, the oxygen-transfer coefficient in the bubble column correlated with the aeration velocity, biomass concentration, and effective viscosity of the broth. The correlations obtained were significantly different for broths with pelleted growth and those with filamentous growth.

1. Introduction

Cholesterol lowering drug lovastatin is commercially produced by submerged culture of the filamentous fungus *Aspergillus terreus* (*A. terreus*).[1,2] Fermentations are usually carried out in stirred tanks. Optimal fermentation medium consists of lactose and soybean meal to provide a C:N mass ratio of ∼70 g g^{-1}, or greater.[3] Use of this medium achieves a lovastatin yield of ∼500 mg (g N)$^{-1}$ within 7 days in an oxygen-rich environment at 28 °C.[3] Maintaining a high concentration of dissolved oxygen is essential for attaining a high titer of lovastatin. Lovastatin production is self-inhibitory.[4]

Growth morphology of the fungus influences lovastatin production.[5,6] In pelleted growth of *A. terreus* in mechanically agitated submerged batch fermentations, the biomass growth profiles are little affected by the agitation tip speed (1.01−2.71 m s^{-1}) or the mode of aeration (air or oxygen enriched gas); however, the agitation speed significantly affects the pellet morphology and lovastatin production. Agitation tip speeds of ≥2.03 m s^{-1} damage fungal pellets of ∼1200 μm initial diameter, reducing them to a final stable pellet diameter of ∼900 μm.[5] At lower agitation speeds, the stable maximum pellet diameter exceeds ∼2500 μm. Pellets of this size produce high lovastatin titers when aerated with oxygen enriched gas but not with air.[5] Much smaller pellets produced under intense agitation (impeller tip speed ≥2.71 m s^{-1}) give poor productivities of lovastatin, irrespective of the mode of aeration used. This suggests that a high oxygen concentration in the pellet is necessary but not sufficient for attaining a high titer of lovastatin. Pellets that are relatively less dense and have a filamentous morphology are better at producing lovastatin compared to small denser pellets. Thus, both an upper limit on acceptable hydrodynamic shear stress and a high oxygen level are indicated for superior production of lovastatin.[5] Hydrodynamic shear forces are known to affect the morphology of numerous other filamentous fungi.[7−12]

We have previously reported on *A. terreus* fermentations conducted in conventional stirred tanks,[5,6] but intense mechanical agitation damaged fungal pellets and reduced production of lovastatin. To circumvent this problem, this work used a gas-agitated slurry bubble column to culture *A. terreus*. The relationships among lovastatin production, pellet morphology, and the broth rheology were studied. The variables investigated were the composition of the aeration gas (standard air or O_2-enriched air), gas flow rate (0.5, 1, and 1.5 vvm), and the concentration of growth-limiting nitrogen source in the medium. The latter was used to influence the biomass concentration attained so that the effects of biomass concentration on fungal broth rheology and pellet development could be assessed.

2. Materials and Methods

2.1. Microorganism and Inoculation. *Aspergillus terreus* ATCC 20542 was obtained from the American Type Culture Collection. The fungus was maintained in Petri dishes of PDA (potato dextrose agar). After inoculation from the original slant, the dishes were incubated at 28 °C for 5 days and subsequently stored at 5 °C. A suspension of spores was obtained by washing the Petri dish cultures with a sterile aqueous solution of 2% Tween 20. The resulting suspension was centrifuged (∼2800*g*, 5 min), and the solids were resuspended in sterile distilled water. The spore concentration was determined spectrophotometrically at 360 nm. A standard curve was used to correlate the optical density to direct spore counts that had been made with a flow cytometer (Coulter Epics XL-MCL).

2.2. Growth Conditions. Fungal pellets were obtained by germination from spores suspended in 250 mL medium in 1000 mL shake flasks held on a rotary shaker (150 rpm, 28 °C, 48

* To whom correspondence should be addressed. E-mail: jlcasas@ual.es.

[†] University of Almeria.

[‡] Massey University.

10.1021/ie0600801 CCC: $33.50
Published on Web 05/18/2006

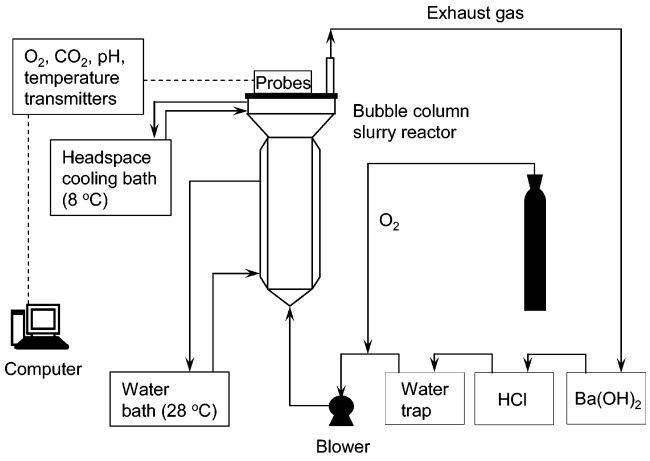

Figure 1. Slurry bubble column bioreactor setup.

h). The initial spore concentration was 3.5×10^6/mL. The culture medium contained lactose as carbon source and soybean meal as nitrogen source. The medium contained the following per liter: 114.26 g of lactose, 5.41 g of soybean meal, 0.8 g of KH_2PO_4, 0.4 g of NaCl, 0.52 g of $MgSO_4 \cdot 7H_2O$, 1 mg of $ZnSO_4 \cdot H_2O$, 2 mg of $Fe(NO_3)_3 \cdot 9H_2O$, 0.04 mg of biotin, and 1 mL of a trace element solution. The trace element solution contained the following (for 1 L of solution): $Na_2B_4O_7 \cdot 10H_2O$, 100 mg; $MnCl_2 \cdot 4H_2O$, 50 mg; $Na_2MoO_4 \cdot 2H_2O$, 50 mg; $CuSO_4 \cdot 5H_2O$, 250 mg. The initial pH was adjusted to 6 with 0.1 M NaOH.

A 900 mL inoculum from the shake flask fermentation stage was used to seed the slurry bubble column bioreactor operated at 28 °C. The medium was the same as that specified above. Fermentations lasted around 8 days.

2.3. Slurry Bubble Column Fermentations. Fermentations were conducted at 28 °C in a 20 L (17 L working volume) bubble column bioreactor with an aspect ratio of 6 (Figure 1). The diameter of the reactor vessel was 0.155 m. Gas was sparged through a perforated plate (150 holes of 1.5 mm diameter) located at the base of the reactor. The gas flow rate was held constant at 0.5, 1.0, or 1.5 vvm in the various runs (Table 1), except during a K_La measurement, as discussed later in this paper. The reactor was fitted with a jacket for temperature control. The top degassing zone of the column had a jacket of its own, and this was cooled at 8 °C to prevent wall growth (Figure 1). Experiments were conducted with air and oxygen-enriched air (80% oxygen) as the sparged gases in different runs (Table 1). When oxygen enriched air was used, the dissolved oxygen concentration in the liquid was controlled at 400% of air saturation. The gas leaving the reactor was recirculated in a closed loop. Prior to recirculation, carbon dioxide was removed by absorption in a $Ba(OH)_2$ solution and pure oxygen was added to maintain the specified oxygen level. Absorption in barium hydroxide ensured that the carbon dioxide concentration in the sparged gas remained at <0.1% (v/v) CO_2. Oxygen and CO_2 partial pressures in the gas stream were measured with on-line sensors (Adaptive Biosystems Ltd., U.K.).

The combinations of various variables studied in different runs (fermentations) are summarized in Table 1. A total of eleven fermentations were conducted under different combinations of conditions. Four of the fermentations were replicates that were used to assess reproducibility.

2.4. Rheological Measurements. Rheological parameters (K, n) were measured using a programmable rotational viscometer (Brookfield DV-II+ with standard vane spindle V-72, 21.7 mm diameter × 43.3 mm height; Brookfield, Middleboro, MA). All measurements were carried out at 28 °C in a glass vessel of 35 mm diameter, filled to 70 mm, following the method described in Casas López et al.[5]

2.5. Morphological Measurements. The fungal pellet morphology was characterized using image analysis.[11] Prior to imaging, each sample of the fermentation broth was processed as follows: 10 mL of sample was decanted and washed twice with 20 mL of distilled water. Within a sample, 100 objects were analyzed for each determination. The image was captured with a CMOS camera (Evolution LC Color; Media Cybernetics, Inc., Silver Spring, MD) mounted on an inverted microscope (Leica DMIL) that used a 40× magnification. Image analysis was performed with the software package Image-Pro Plus 4.5.1 (Media Cybernetics, Inc., Silver Spring, MD).

The changes in pellet morphology were quantified using the following two measures: (1) the diameter corresponding to a circular area equivalent to the total pellet projected area, as a one-dimensional measurement of the pellet size; and (2) the ratio between the area of the peripheral "hairy surface" and the total area of the pellet. This ratio was termed the "filament ratio". These two measures provided a direct indication of the pellet size and the proportion of filamentous growth in it. For instance, in the early stages of fermentation, a young pellet would be typically characterized by a small diameter and a filament ratio close to 100%. As fermentation progressed, the filament ratio would reduce.

2.6. Gas−Liquid Mass-Transfer and Specific Oxygen Uptake Rate Measurements. The overall gas−liquid volumetric mass-transfer coefficient K_La and oxygen uptake rate (OUR) were measured using a modified dynamic gassing in method,[13] involving an oxygen mass balance. The modified dynamic method used did not require any change to the flow rate of the aeration gas.[14] An instantaneous step change in the composition of the aeration gas (i.e. air to pure oxygen) was used exclusively to alter the mass-transfer driving force, so that the hydrodynamic regimen in the bubble column was not disturbed during the measurement. The flow rate of the aeration gas was measured by a mass flow meter (Omega FMA-1800).

The dissolved oxygen concentration was measured using a polarographic electrode (Mettler Toledo; InPro 6100/220T). Electrode characteristics can influence the K_La measurements;[13,15] therefore, the electrode response dynamics were characterized experimentally. A first-order response with time delay was observed; thus,

$$C_L(t - t_d) = C_E(t) + \frac{1}{k}\frac{dC_E(t)}{dt} \quad (1)$$

where C_L is the concentration of dissolved oxygen at time t, $C_E(t)$ is the electrode response signal at time t, t_d is the delay time, and k is a time constant. The dissolved oxygen readings were corrected to take into account the delay time ($t_d = 5.2 \pm$

Table 1. Specific Conditions Used in the Various Fermentation Runs in the Bubble Column

	run I	run II	run III	run IV	run V	run VI	run VII	run VIII	run IX	run X	run XI
nitrogen (g L^{-1})	0.15	0.15	0.15	0.15	0.15	0.15	0.46	0.46	0.92	0.92	0.92
gas flow rate (vvm)	1.0	1.0	1.0	0.5	1.5	1.5	1.0	1.0	1.0	1.0	1.0
gas-phase composition	air	air	80% O_2	80% O_2	80% O_2	80% O_2	80% O_2	80% O_2	80% O_2	80% O_2	air

0.2 s at 95% confidence level) and the time constant ($k = 0.064 \pm 0.004$ s^{-1} at 95% confidence level).

The dissolved oxygen concentration was monitored as a function of time. Once the medium was close to saturation with oxygen, the composition of the aeration gas reverted to that of air and the desorption step commenced.

The $K_L a$ and OUR values were obtained as the parameters that provided the best fit of the measured dissolved oxygen concentration profile to the profile generated with the following equation:

$$C_L = \left(C^* - \frac{C_b \mathrm{OUR}}{K_L a}\right) + \left(C_{L0} - C^* + \frac{C_b \mathrm{OUR}}{K_L a}\right) e^{-K_L a t} \quad (2)$$

where C^* is the saturation concentration of dissolved oxygen, C_{L0} is the initial concentration of dissolved oxygen, and C_b is the biomass concentration. Equation 2 is the integrated form of the dynamic mass balance of oxygen, i.e.,

$$\frac{dC_L}{dt} = K_L a(C^* - C_L) - C_b \mathrm{OUR} \quad (3)$$

2.7. Analytical Methods. 2.7.1. Biomass. The biomass (as dry weight) was determined by filtering a known volume of the broth through a 0.45 μm Millipore cellulose filter, washing the cells with sterile distilled water, and freeze-drying the solids.

2.7.2. Lovastatin. Lovastatin was measured in its β-hydroxy acid form by HPLC of the biomass-free filtered broth.[16,17] The filtered broth containing the β-hydroxy acid was diluted 10-fold with acetonitrile/water (1:1, v/v) prior to analysis. Pharmaceutical-grade lovastatin (lactone form) tablets (Nergadan tablets; J. Uriach and Cía., S. A.) were used to prepare the standards for HPLC analyses. Prior to use, the lactone form was converted into its β-hydroxy acid form by dissolving the tablets in a mixture of 0.1 N NaOH and ethanol (1:1, v/v), heating the solution at 50 °C for 20 min, and neutralizing it with HCl. HPLC was done on a Beckman Ultrasphere ODS (250 × 4.6 mm i.d., 5 μm) column. The column was mounted in a Shimadzu model LC10 liquid chromatograph equipped with a Shimadzu MX-10Av diode array detector. The eluent was a mixture of acetonitrile and 0.1% phosphoric acid (60:40, v/v). The eluent flow rate was 1.5 mL min^{-1}. The detection wavelength was 238 nm. The sample injection volume was 20 μL.

3. Results and Discussion

Biomass concentration in batch runs I−XI increased with fermentation time irrespective of the composition of the gas used for sparging the culture (Figure 2). The final biomass concentration depended on the initial nitrogen concentration in the medium. For example, in runs I−VI the final biomass concentration was near 3.2 g L^{-1} (Figure 2) for a nitrogen concentration of 0.15 g L^{-1} (Table 1). Runs VII and VIII attained a biomass concentration of 8.9 g·L^{-1} because of an elevated initial nitrogen level of 0.46 g L^{-1} (Table 1). Maximum biomass concentration rose to 18.0 g L^{-1} (runs IX, X, and XI, Figure 2) when the initial nitrogen concentration in the medium was 0.92 g L^{-1}. In all cases, the biomass yield was close to the theoretical yield on nitrogen, i.e., 21 g of biomass/(g of N).[3] Increasing initial concentration of N in the medium delayed the onset of the stationary phase from approximately at 75 h to as late as 200 h (Figure 2). Data in Figure 2 suggest that oxygen was not a growth limiting factor in any of the runs I−XI.

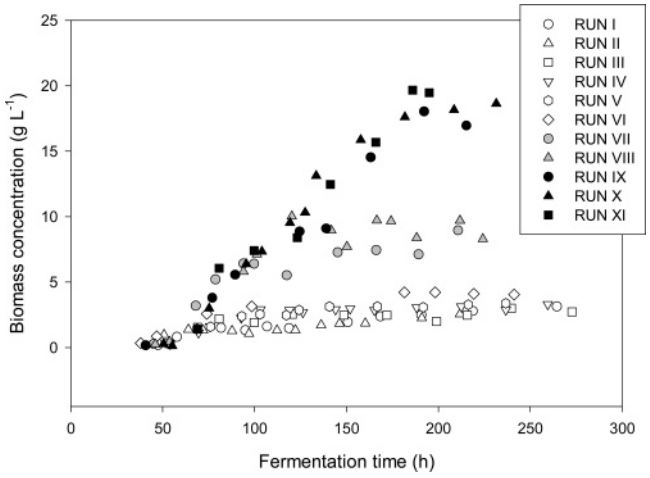

Figure 2. Biomass concentration versus fermentation time.

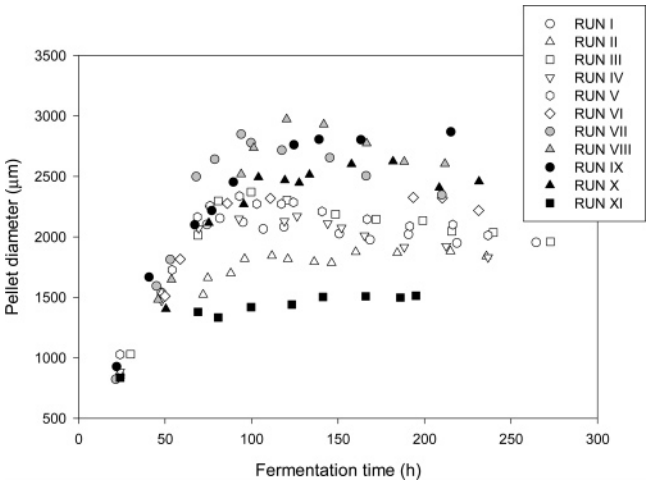

Figure 3. Pellet morphology: diameter versus fermentation time.

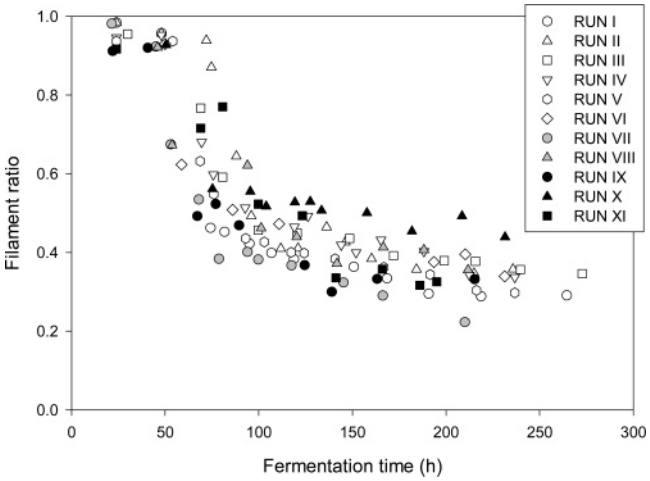

Figure 4. Pellet morphology: filament ratio versus fermentation time.

The fungal pellet morphology as characterized by the mean pellet diameter and filament ratio varied with fermentation time, as shown in Figures 3 and 4. In general, the pellet diameter was not affected much by the aeration rate but was influenced more by the gas composition used (Table 1). Sparging with normal air gave rise to smaller pellets than were obtained in oxygen-rich environments, especially at the highest nitrogen level (run XI). In the latter case, filamentous mycelial morphology was predominant and accounted for 85% of the total fungal biomass.

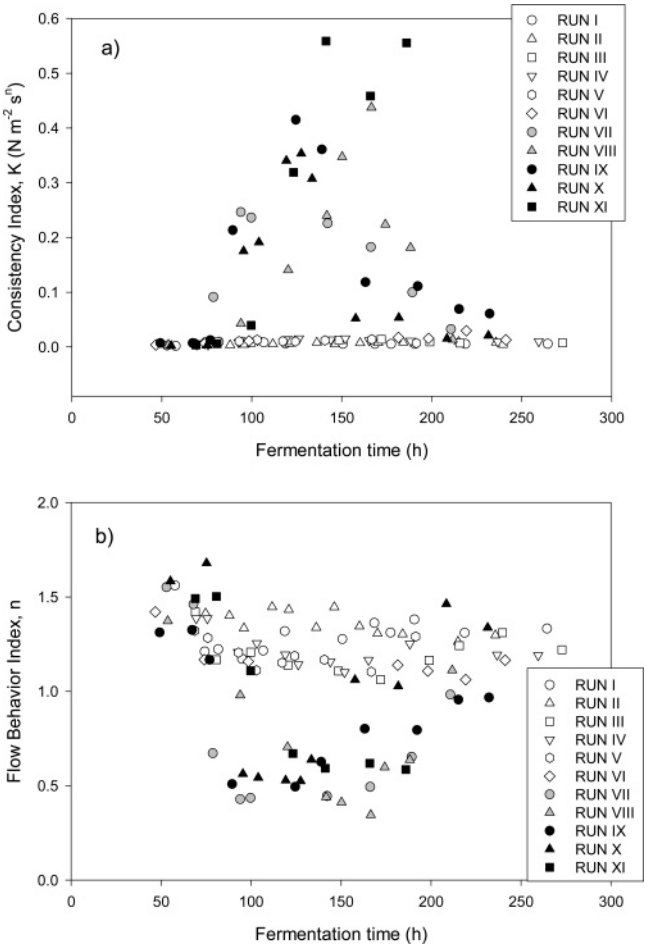

Figure 5. Consistency index (a) and flow behavior index (b) of the broth at various times during fermentation.

In all cases, the mean pellet diameter increased for the first 75 h of fermentation until a stable pellet diameter was attained. Pellet size did not increase further, even though the biomass concentration in the broth continued to increase. Erosion of the pellets prevented a further increase in size.

At the two highest nitrogen levels tested (i.e. runs VII−X, Table 1) the final stable pellet size of ∼2700 μm was significantly larger than the 2300 μm final size attained in low-nitrogen runs (i.e., runs I−VI; Figure 3) Furthermore, at the highest nitrogen level (i.e. 0.92 g L^{-1}; runs IX and X) the pellets size did not decline slightly as occurred in the lower-nitrogen runs (Figure 3). This suggests that decline in size seen in the low nitrogen runs was associated with erosion in the absence of ongoing biomass generation because of nitrogen limitation. In the absence of nitrogen limitation, the biomass growth compensated to some degree for the loss by erosion. The filament ratio was initially around 95% in all cases (Figure 4), but subsequently declined to around 40%. The hydrodynamic regime in the bioreactor caused pellets to grow as compact dense particles in which the outer protruding hyphae were being forced to grow into the pellet.

Rheological behavior of the bulk broth fitted to the Ostwald−deWaelle's power law model. Figure 5 shows the *K*- and *n*-values of the broth at different stages of the fermentation in the various runs. A comparison of Figs 2, 3, and 5 reveals that the broth rheology was being affected both by the biomass concentration and the pellet size. Low-N fermentations that attained relatively low biomass concentrations (i.e., runs I−VI in Figure 5a) had a low value of *K* all through the fermentation.

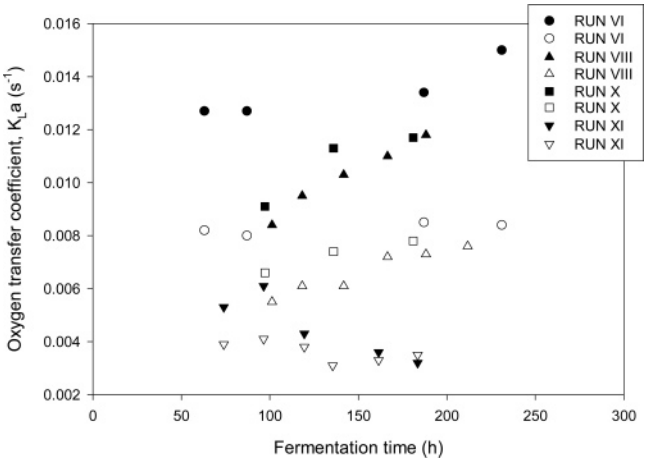

Figure 6. K_La measured at two superficial gas velocities versus fermentation time: $U_g = 0.014$ m s^{-1} (open symbols) and $U_g = 0.021$ m s^{-1} (solid symbols).

In runs VII−X, the *K*-value increased as the biomass concentration increased, but only until ∼100 h when the pellets attained a relatively constant size. This suggests that increasing size of pellets strongly influenced the *K*-value but *K* was not sensitive to an increase in the concentration of pellets of a fixed diameter. Run XI presented a different rheological behavior because of a predominantly filamentous mycelial morphology. The consistency index increased with increasing biomass concentration and remained at its maximum value until the end of the run. The culture bulk was highly viscous in comparison with the pelleted cultures that had the same biomass concentration.

In both low-N and high-N runs, the *n*-value initially declined as the fermentation progressed (Figure 5b). The high-N broths became highly pseudoplastic ($n < 1$) during the first 75−100 h from an initial dilatant ($n > 1$) behavior as they attained much higher biomass concentrations than did the low-N broths. Subsequently, the *n*-value of high-N broths increased with fermentation time. This was because by 100 h the pellet diameter had stabilized near its maximum value but the concentration of pellets continued to increase. These observations about the effects of pellet morphology on broth rheology are consistent with similar behavior that has been reported in mechanically agitated tank cultures of *A. terreus*.[5,6] Once again, the predominantly filamentous broth of run XI had a different behavior compared with the broth of runs IX and X. The flow behavior index declined during the first 120 h (run XI) and remained at around 0.6 until the end of the fermentation.

The availability of oxygen is known to play a significant role in lovastatin production by *A. terreus*. In a bubble column reactor of a given configuration, mass transfer of oxygen depends on the rheology of the fluid, the gas−liquid interfacial tension, and the superficial velocity of the aeration gas. Interfacial tension was discounted in this study as an influencing variable because the various fermentation broths all had a fairly constant surface tension value of 28.1 ± 1.0 mN m^{-1} (at 95% confidence interval), and surface tension variation during a fermentation was negligible. Figure 6 shows the K_La values measured at various times in selected fermentation runs that ranged in biomass concentrations from low to high and broth morphology from pelleted to filamentous. For each run, K_La was measured at two different values of the superficial aeration velocity (Figure 6).

The low-N culture (run VI) produced a low-viscosity broth and relatively steady values of K_La during the fermentation. In every case, the K_La values increased with an increase in the

Table 2. Values of Parameters *a*, *b*, *c*, and *d* in Equation 4 for the Two Growth Morphologies

morphology ↓	a	b	c	d	$r^{2\,a}$
pellet growth	0.43	0.95	−0.03	−0.03	0.90
filamentous growth	0.15	0.74	−0.01	−0.20	0.91

[a] r^2 = determination coefficient.

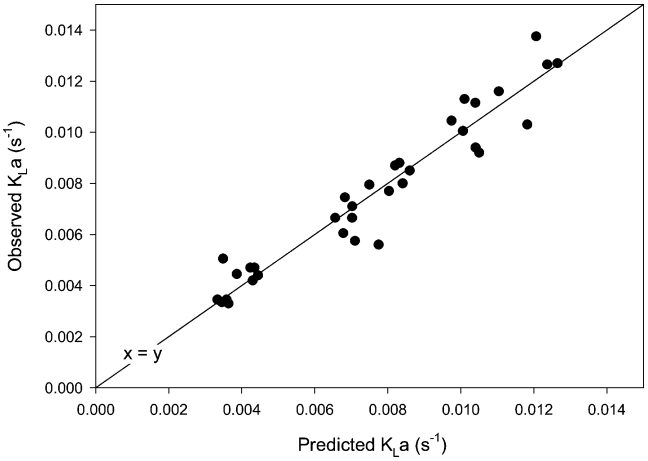

Figure 7. Parity plot comparison of model predicted K_La and experimental data.

aeration velocity because of increased turbulence and a reduced bubble size. Broths that had a predominantly pelleted morphology produced higher K_La values compared with the run XI broth that had a predominantly filamentous morphology. This behavior is consistent with many other similar observations,[8,18] and it occurs because the prevailing bubble size in highly viscous filamentous broths is generally larger than in less viscous, more turbulent, pelleted broths.

The overall gas−liquid oxygen-transfer coefficient, K_La, was fitted to the following equation:

$$K_La = aU_g^{\,b}\mu_{ef}^{\,c}C_b^{\,d} \tag{4}$$

where U_g is the superficial gas velocity (m s^{-1}), μ_{ef} is "effective" viscosity, C_b is the biomass concentration (kg m^{-3}), and *a*, *b*, *c*, and *d* are experimentally fitted parameters. In keeping with the literature on bubble columns and airlift bioreactors, the effective viscosity for use in the above equation was defined as follows:

$$\mu_{ef} = KU_g^{\,n-1} \tag{5}$$

where *K* and *n* were the consistency index and the flow behavior index of the fluid, respectively. The parameters *a*, *b*, *c*, and *d* had the values shown in Table 2.

Figure 7 compares the K_La values predicted with eq 4 and the experimentally measured data. The mean absolute error of the predictions was 7.4×10^{-4}. The superficial gas velocity was the major influence on K_La, but broth rheology-associated factors also had an influence (Table 2). Compared to eq 4, other authors have reported a stronger influence of apparent viscosity on K_La [19,20] in broths that generally focused on simulating the filamentous fungal morphology. As has been pointed out in the past, the value of the exponent *c* (eq 4) is influenced by the definition of shear rate in slurry bubble columns and other pneumatically agitated bioreactors, but there is no general consensus about the precise value of the shear rate that exists in these reactors.[12,21]

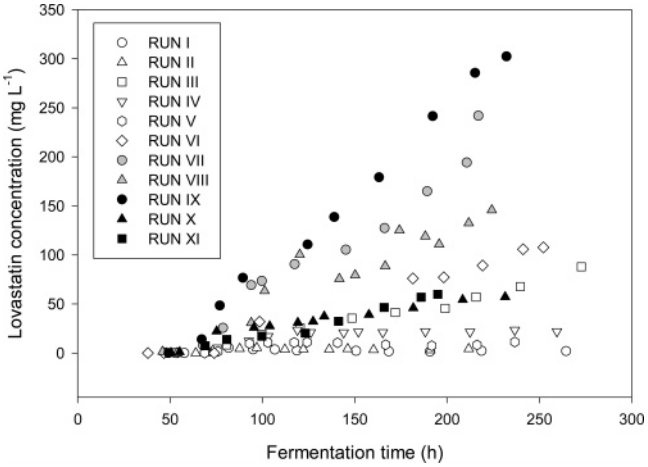

Figure 8. Lovastatin concentration profiles versus fermentation time.

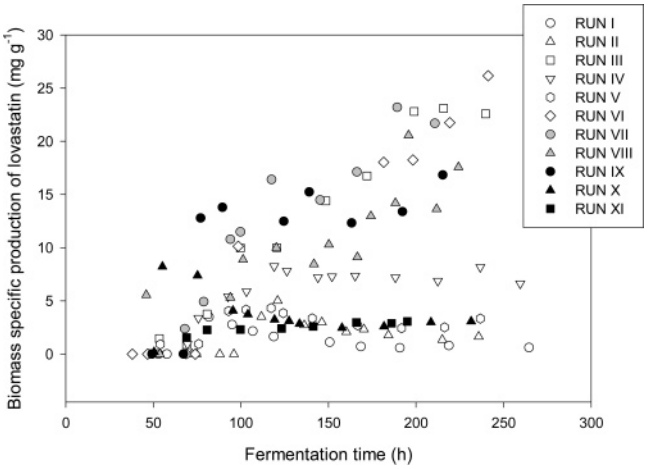

Figure 9. Biomass-specific production of lovastatin during fermentation.

Lovastatin concentration profiles for the various runs are shown in Figure 8. A comparison of Figure 8 with the biomass concentration profiles (Figure 2) for the same runs revealed that in general higher titers of lovastatin were attained in high-N runs that also attained high concentrations of biomass. The biomass-specific production of lovastatin (Figure 9) of the high-biomass, high-N, runs was generally substantially higher than for the other runs, except run IV. Runs I, II, and XI had a low biomass-specific production of lovastatin because sparging with normal air produced only a relatively low level of dissolved oxygen. Run IV was also relatively low in dissolved oxygen because the sparging rate was low at 0.5 vvm (Table 1). Consequently, run IV had a low production of lovastatin. Runs V and X had anomalously low production of lovastatin because of poor starting inocula. In view of these results, good biomass-specific production and high bioreactor productivity of lovastatin require both an oxygen-rich environment that is not excessively agitated and a high biomass concentration that is attained by providing high levels of nitrogen.

Figure 10 shows the specific oxygen uptake rate (mmol g^{-1} h^{-1}) values observed at various stages during the fermentation for selected runs (runs V, VIII, X, and XI). Data were similar for the other runs. In all cases, a high initial OUR value of around 1 mmol g^{-1} h^{-1} indicated a vigorous culture under optimal conditions of growth. OUR declined rapidly with the progress of fermentation, and by around 100 h the OUR value was ≤0.5 mmol g^{-1} h^{-1}. Near the end of the fermentations the OUR value had declined to <0.2 mmol g^{-1} h^{-1}, indicating a slowed metabolism of the fungus.

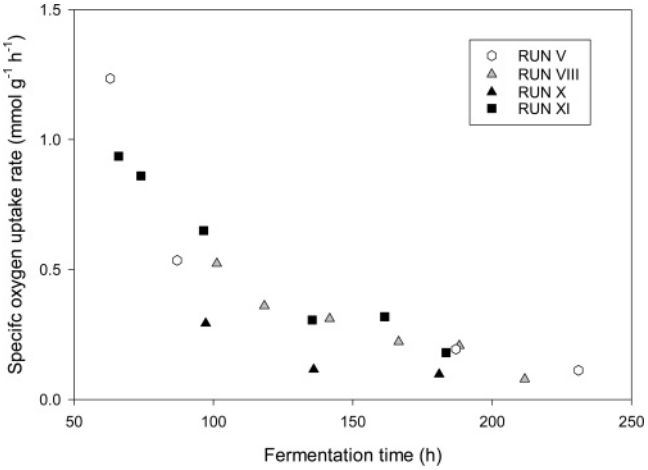

Figure 10. Specific oxygen uptake rate during various fermentations.

The profiles shown in Figure 10 include cultures that had very different biomass concentrations and were aerated with different compositions of the aeration gas. Similar variation of OUR with fermentation time in fermentations that were quite diverse suggests that the primary metabolism (i.e., cell growth) was not particularly sensitive to oxygen concentration so long as the concentration was close to or above the air-saturation value. However, the secondary metabolism (i.e., synthesis of lovastatin) responded positively to elevated concentrations of dissolved oxygen. Thus, within the experimental space, the OUR had no influence on production of lovastatin. This suggests that the synthesis of lovastatin is sensitive to the concentration of dissolved oxygen and not to OUR.

Molecular oxygen is required in the biosynthesis of lovastatin molecules via the polyketide pathway,[22,23] and an elevated dissolved oxygen concentration probably affects some equilibrium step in the biosynthetic route, to enhance the final lovastatin concentration. The results clearly confirm that oxygen availability has an important role in lovastatin production and that the dissolved oxygen in the fermentation broth should be controlled for attaining a high productivity of lovastatin [3].

4. Concluding Remarks

High lovastatin titers, biomass specific lovastatin production, and bioreactor productivity are attained under oxygen-rich conditions in the bubble column at 1 vvm gas sparging rate. Sparging with normal air is insufficient for attaining high titers of lovastatin. Increasing the biomass concentration in the reactor by increasing the supply of growth limiting nitrogen source does not affect the stable fungal pellet size substantially, but the concentration of pellets is increased at a given sparging rate in the reactor. In comparison with other published data for the same fermentation in stirred bioreactors,[5] slurry bubble columns appear to be better for culturing *A. terreus*. In *A. terreus* broths, the oxygen-transfer coefficient in the bubble column depends on the aeration velocity, biomass concentration, and the effective viscosity of the broth; however, this dependence is substantially affected by whether the biomass is present in predominantly pelleted form or in filamentous growth.

Acknowledgment

This research was supported by the Ministerio de Educación y Ciencia (Grant CTQ2004-04454/PPQ) and Junta de Andalucía, PAI III (Grant CVI 263).

Nomenclature

C^* = saturation concentration of dissolved oxygen (mmol L^{-1})
C_{L0} = initial concentration of dissolved oxygen (mmol L^{-1})
C_b = biomass concentration (g L^{-1})
$C_E(t)$ = oxygen electrode response signal at time t (mmol L^{-1})
C_L = concentration of dissolved oxygen (mmol L^{-1})
a = parameter in eq 4
b = parameter in eq 4
c = parameter in eq 4
d = parameter in eq 4
K = consistency index (Pa s^n)
K_La = overall gas−liquid volumetric mass-transfer coefficient (s^{-1})
k = electrode time constant (s)
n = flow index
OUR = specific oxygen uptake rate (mmol g^{-1} s^{-1})
t = time (s)
t_d = delay time (s)
U_g = superficial gas velocity (m s^{-1})

Greek Symbols

μ_{ef} = effective viscosity (Pa s)

Literature Cited

(1) Gbewonyo, K.; Hunt, G.; Buckland, B. Interactions of cell morphology and transport processes in the lovastatin fermentation. *Bioprocess Eng.* **1992**, *8*, 1−7.

(2) Tobert, J. A. Lovastatin and beyond: The history of the HMG-CoA reductase inhibitors. *Nat. Rev. Drug Discovery* **2003**, *2*, 517−526.

(3) Casas López, J. L.; Sánchez Pérez, J. A.; Fernández Sevilla, J. M.; Acién Fernández, F. G.; Molina Grima, E.; Chisti, Y. Fermentation optimization for the production of lovastatin by *Aspergillus terreus*: Use of the response surface methodology. *J. Chem. Technol. Biotechnol.* **2004**, *79*, 1119−1126.

(4) Casas López, J. L.; Rodríguez Porcel, E. M.; Vilches Ferrón, M. A.; Sánchez Pérez, J. A.; Fernández Sevilla, J. M.; Chisti, Y. Lovastatin inhibits its own synthesis in *Aspergillus terreus*. *J. Ind. Microbiol. Biotechnol.* **2004**, *31*, 48−50.

(5) Casas López, J. L.; Sánchez Pérez, J. A.; Fernández Sevilla, J. M.; Rodríguez Porcel, E. M.; Chisti, Y. Pellet morphology, culture rheology and lovastatin production in cultures of *Aspergillus terreus*. *J. Biotechnol.* **2005**, *116*, 61−77.

(6) Rodríguez Porcel, E. M.; Casas López, J. L.; Sánchez Pérez, J. A.; Fernández Sevilla, J. M.; Chisti, Y. Effects of pellet morphology on broth rheology in fermentations of *Aspergillus terreus*. *Biochem. Eng. J.* **2005**, *26*, 139−144.

(7) Metz, B.; Kossen, N. W. F. The growth of molds in the form of pellets−A literature review. *Biotechnol. Bioeng.* **1977**, *19*, 781−799.

(8) Metz, B.; Kossen, N. W. F.; van Suijdam, J. C. The rheology of mold suspensions. *Adv. Biochem. Eng.* **1979**, *11*, 103−156.

(9) Jüsten, P.; Paul, G. C.; Nienow, A. W.; Thomas, C. R. Dependence of mycelial morphology on impeller type and agitation intensity. *Biotechnol. Bioeng.* **1996**, *52*, 672−684.

(10) Jüsten, P.; Paul, G. C.; Nienow, A. W.; Thomas, C. R. Dependence of *Penicillium chrysogenum* growth, morphology, vacuolation and productivity in fed-batch fermentations on impeller type and agitation intensity. *Biotechnol. Bioeng.* **1998**, *59*, 762−775.

(11) Paul, G. C.; Thomas, C. R. Characterisation of mycelial morphology using image analysis. *Adv. Biochem. Eng.* **1998**, *60*, 1−59.

(12) Chisti, Y. Shear sensitivity. In *Encyclopedia of Bioprocess Technology: Fermentation, Biocatalysis, and Bioseparation*, Vol. 5; Flickinger, M. C., Drew, S.W., Ed.; Wiley: New York, 1999; pp 2379−2406.

(13) Van't Riet, K. Review of measuring methods and results in nonviscous gas−liquid mass transfer in stirred vessels. *Ind. Eng. Process Des. Dev.* **1979**, *18*, 357−364.

(14) Casas López, J. L.; Rodríguez Porcel, E. M.; Oller Alberola, I.; Ballesteros Martin, M. M., J. A. Sánchez Pérez, J. A.; Fernández Sevilla, J. M.; Chisti, Y. Simultaneous determination of oxygen consumption rate and volumetric oxygen transfer coefficient in pneumatically agitated bioreactors. *Ind. Eng. Chem. Res.* **2006**, *45*, 1167−1171.

(15) Juárez, P.; Orejas, J. Oxygen transfer in a stirred reactor in laboratory scale. *Lat. Am. Appl. Res.* **2001**, *31*, 433−439.

(16) Friedrich, J.; Zuzek, M.; Bencina, M.; Cimerman, A.; Strancar, A.; Radez, I. High-performance liquid chromatographic analysis of mevinolin as mevinolinic acid in fermentation broths. *J. Chromatogr., A* **1995**, *704*, 363−367.

(17) Morovján, G.; Szakács, G.; Fekete, J. Monitoring of selected metabolites and biotransformation products from fermentation broths by high-performance liquid chromatography. *J. Chromatogr., A* **1997**, *763*, 165−172.

(18) Chisti, Y. Mass transfer. In *Encyclopedia of Bioprocess Technology: Fermentation, Biocatalysis, and Bioseparation*, Vol. 3; Flickinger, M.C., Drew, S. W., Ed.; Wiley: New York, 1999; pp 1607−1640.

(19) Kawase, Y.; Moo-Young, M. Influence of non-newtonian flow behavior on mass transfer in bubble columns with and without draft tubes. *Chem. Eng. Commun.* **1986**, *40*, 67−83.

(20) Pavko, A. Gas/liquid oxygen mass transfer in bubble columns and modified bubble columns. *Chem. Biochem. Eng. Q.* **1989**, *3*, 33.

(21) Chisti, Y.; Moo-Young, M. On the calculation of shear rate and apparent viscosity in airlift and bubble column bioreactors. *Biotechnol. Bioeng.* **1989**, *34*, 1391−1392.

(22) Wagschal, K.; Yoshizawa, Y.; Witter, D. J.; Liu, Y.; Vederas, J. C. Biosynthesis of ML-236C and the hypocholesterolemic agents compactin by *Penicillium aurantiogriseum* and lovastatin by *Aspergillus terreus*: Determination of the origin of carbon, hydrogen, and oxygen atoms by 13-C NMR spectrometry and observation of unusual labeling of acetate-derived oxygens by 18-O_2. *J. Chem. Soc., Perkin Trans.* **1996**, *1* (19), 2357−2363.

(23) Yoshizawa, Y.; Witter, D. J.; Liu, Y.; Vederas, J. C. Revision of the biosynthetic origin of oxygens in mevinolin (lovastatin), a hypocholesterolemic drug from *Aspergillus terreus* MF 4845. *J. Am. Chem. Soc.* **1994**, *116*, 2693−2694.

Received for review January 18, 2006
Revised manuscript received March 31, 2006
Accepted April 19, 2006

IE0600801